Nonlinear Estimation of Stator Winding Resistance in a Brushless DC Motor

Wanlin Zhang, S. Andrew Gadsden, and Saeid R. Habibi

***Abstract*—Estimation of stator winding resistance in brushless DC motors is important for fault detection and diagnosis. The most popular linear estimation method to date remains the Kalman filter (KF), and the extended form (EKF) for nonlinear systems and measurements. However, a relatively new method referred to as the smooth variable structure filter (SVSF) was introduced in an effort to overcome some of the instability issues with the KF. Further to this development, a new nonlinear estimation strategy was created based on combining elements of the EKF with the SVSF. This new method, referred to as the EK-SVSF, has been applied to a brushless DC motor for estimating the stator winding values. The results are compared with the popular EKF.**

I. Introduction

Electric motors are an essential part of many production and manufacturing lines, with increasing popularity in the automotive, aerospace, HVAC, and medical fields. One of the most common types of electric motors is referred to as the permanent magnet brushless DC motor (PMBLDC). Unplanned production downtime caused by motor failures greatly affects production costs and operator safety.

Stator winding faults, namely open phase and short-circuited phase, account for nearly 21% of motor failures [1, 2]. Therefore, it is important to implement effective fault diagnosis techniques in order to detect failures at the inception. Winding failure most commonly starts as turn-to-turn faults, and develops to the open phase or insulation failure. This causes the motor parameters such as the winding resistance to vary [2]. Mathematical models of electric motors are used to estimate and monitor the parameters in order to identify the potential deterioration of winding conditions. Model-based estimation methods provide a nonintrusive and low-cost way to monitor motor operating conditions [3-8].

A parametric model was developed to simulate the operating conditions in [9], where the variation of spatial harmonics in back-EMFs was taken into account. A similar approach was also used in [10]. In [11] a sliding-mode observer was proposed to estimate the back-EMF of a brushless DC motor, and was found insensitive to switching noise in the power measurements. The extend Kalman filter (EKF) has become one of the favored approaches for the estimation of motors, such as rotor position in sensorless control [12, 13]. In [14] the faults in the winding resistance and the friction coefficient of a brushless DC motor were physically simulated and estimated using EKF. The results demonstrated that a 10% winding resistance fault could be overcome. However, the study did not consider a signal winding phase fault case.

In [15] a model-reference based method was proposed for the parameter estimation of a motor. It was claimed that the performance of the proposed approach was comparable to that of EKF [16], while being less computationally expensive. The EKF was also employed in [17] for the estimation of rotor speed and winding resistance of a brushless DC motor. The accuracy of the estimated speed could be improved by introducing the estimation of winding resistance. The EKF has also been implemented for estimating sensorless stepper motor drives with long cables; two estimation schemes for a motor side and drive side were developed combined [18]. A fault diagnosis algorithm was proposed in [19] which accounted for the modeling errors caused by process uncertainties. The uncertainties were reflected by a time-varying stator resistance and inductance. The approach utilized a decoupling block formulated in a feedback loop to increase the overall robustness. However, the studied assumed that the winding resistances of all three phases were equal to each other, which is not practical under faulty winding conditions.

Model-based approaches often have issues with overlooked modeling uncertainties and nonlinearities that can lead to incorrect or unstable estimates [20]. In 2007, a new strategy referred to as the smooth variable structure filter (SVSF) was introduced in an effort to improve the resistance to modeling errors [21]. It was proved that it could guarantee stability given some bounded parametric uncertainty [21]. An improved version of the SVSF, referred to as the EK-SVSF, was proposed in [22]. It achieves better estimation accuracy by making use of the EKF while also preserving the robustness features of the SVSF. In this study, the EK-SVSF was adopted for estimating the winding resistance of a brushless DC Motor. The main EKF, SVSF, and EK-SVSF equations are summarized in Section's 2 and 3. The experimental setup and results are provided in Section 4. Finally, the results are summarized in the conclusions.

II. Estimation Strategies

A. Extended Kalman Filter

The extended Kalman filter (EKF) for nonlinear systems and measurements is similar to the standard KF; however it makes use of linearized system and measurement matrices. The state estimate $\hat{x}_{k+1|k}$ is predicted using the nonlinear system model (2.1.1), and the corresponding state error covariance matrix $P_{k+1|k}$ is calculated as per (2.1.2). The measurement error (or innovation) $e_{z,k+1|k}$ is calculated using (2.1.3), and the measurement error (innovation) covariance matrix S_{k+1} is calculated by (2.1.4).

W Zhang, S. A. Gadsden, and S. R. Habibi are with the Department of Mechanical Engineering, McMaster University, Hamilton, Ontario, Canada, L8S 4L7 (e-mails: zhangw53@mcmaster.ca, gadsden@mcmaster.ca and habibi@mcmaster.ca).

$$\hat{x}_{k+1|k} = f(\hat{x}_{k|k}, u_k) \quad (2.1.1)$$
$$P_{k+1|k} = A_k P_{k|k} A_k^T + Q_k \quad (2.1.2)$$
$$e_{z,k+1|k} = z_{k+1} - h(\hat{x}_{k+1|k}) \quad (2.1.3)$$
$$S_{k+1} = C_{k+1} P_{k+1|k} C_{k+1}^T + R_{k+1} \quad (2.1.4)$$

The gain is calculated next as per (2.1.5), making use of (2.1.2) and (2.1.4). An updated state estimated is calculated in (2.1.6) based on the measurement error (2.1.3) and the gain. Finally, the state error covariance matrix is updated in (2.1.7) and used in the next time step.

$$K_{k+1} = P_{k+1|k} C_{k+1}^T S_{k+1}^{-1} \quad (2.1.5)$$
$$\hat{x}_{k+1|k+1} = \hat{x}_{k+1|k} + K_{k+1} e_{z,k+1|k} \quad (2.1.6)$$
$$P_{k+1|k+1} = (I - K_{k+1} C_{k+1}) P_{k+1|k} \quad (2.1.7)$$

Equations (2.1.1) through (2.1.7) are the main equations for the EKF estimation process. Note that the process is performed recursively. Furthermore, for completeness, the linearized system and measurement matrices may be calculated respectively as follows:

$$A_k = \left.\frac{\partial f}{\partial x}\right|_{\hat{x}_{k|k}, u_k} \quad (2.1.8)$$
$$C_{k+1} = \left.\frac{\partial h}{\partial x}\right|_{\hat{x}_{k+1|k}} \quad (2.1.9)$$

B. *Smooth Variable Structure Filter*

As previously discussed, the smooth variable structure filter (SVSF) is a relatively new estimation method based on sliding mode concepts [21]. Like the KF and EKF, the SVSF is formulated in a predictor-correct format. The unique switching gain that the SVSF utilizes creates a very robust and stable estimation strategy [21]. As illustrated in Fig. 1, a switching gain is used to force the estimates to within a region of the true state trajectory, referred to as the existence subspace. The width of this boundary layer is a function of the modeling errors and uncertainties present in the estimation process. Properly identifying these levels of uncertainties and noise creates a robust and accurate estimation method [21].

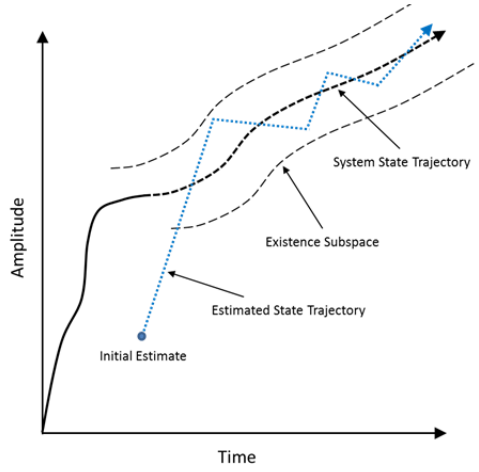

Figure 1. SVSF estimation concept [23].

The SVSF estimation process may be summarized by the following set of equations. Similar to the EKF process, the state estimates (2.2.1), state error covariance matrix (2.2.2), and a priori measurement error (2.2.3) are calculated first in the prediction step.

$$\hat{x}_{k+1|k} = f(\hat{x}_{k|k}, u_k) \quad (2.2.1)$$
$$P_{k+1|k} = A_k P_{k|k} A_k^T + Q_k \quad (2.2.2)$$
$$e_{z,k+1|k} = z_{k+1} - h(\hat{x}_{k+1|k}) \quad (2.2.3)$$

The SVSF gain is a function of: the a priori and a posteriori measurement errors $e_{z,k+1|k}$ and $e_{z,k|k}$; the smoothing boundary layer widths ψ; the 'SVSF' memory or convergence rate γ; as well as the linearized measurement matrix C; and is defined as per (2.2.4). Similar to the EKF process, the gain is used to update the state estimate (2.2.5) and update the state error covariance matrix (2.2.6).

$$K_{k+1} = C^+ diag\left[\left(\left|e_{z_{k+1|k}}\right| + \gamma\left|e_{z_{k|k}}\right|\right) \circ sat\left(\bar{\psi}^{-1} e_{z_{k+1|k}}\right)\right] diag\left(e_{z_{k+1|k}}\right)^{-1} \quad (2.2.4)$$
$$\hat{x}_{k+1|k+1} = \hat{x}_{k+1|k} + K_{k+1} e_{z,k+1|k} \quad (2.2.5)$$
$$P_{k+1|k+1} = (I - K_{k+1}C) P_{k+1|k} (I - K_{k+1}C)^T + K_{k+1} R_{k+1} K_{k+1}^T \quad (2.2.6)$$

The measurement error, used in the next time step, is updated as per (2.2.7).

$$e_{z,k+1|k+1} = z_{k+1} - h(\hat{x}_{k+1|k+1}) \quad (2.2.7)$$

III. The EK-SVSF Estimation Strategy

Recently, it was proposed to combined elements of the EKF and SVSF to improve the overall estimation accuracy and robustness [23]. This procedure is based on a time-varying smoothing boundary layer (VBL), as opposed to a fixed smoothing boundary layer value (used to define the existence subspace). Essentially, the VBL may be used as an indicator of system changes or fault occurrences. The combined method, referred to as the EK-SVSF, makes use of the VBL and the fixed or saturated boundary layer width. The EKF gain is implemented if the VBL is calculated to exist within (or less than) the fixed value. If the VBL goes beyond the limit, the SVSF gain is implemented in order to maintain robustness to modeling uncertainties and noise. This concept is further illustrated in Fig. 2.

The EKF-SVSF estimation process is summarized by the following set of equations. The prediction stage begins as per the EKF method.

$$\hat{x}_{k+1|k} = f(\hat{x}_{k|k}, u_k) \quad (3.1)$$
$$P_{k+1|k} = A_k P_{k|k} A_k^T + Q_k \quad (3.2)$$
$$e_{z,k+1|k} = z_{k+1} - h(\hat{x}_{k+1|k}) \quad (3.3)$$
$$S_{k+1} = C_{k+1} P_{k+1|k} C_{k+1}^T + R_{k+1} \quad (3.4)$$

At this point, the time-varying smoothing boundary layer (VBL) is calculated as follows [23]:

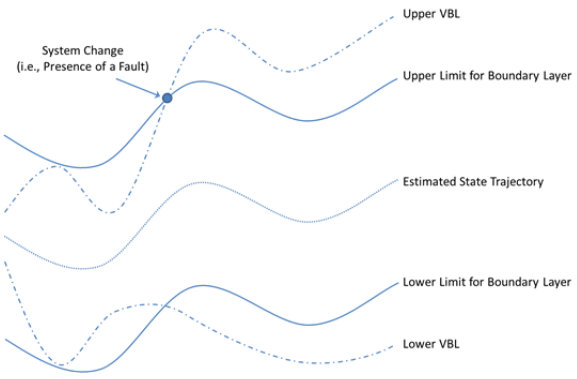

Figure 2. Time-varying smoothing boundary layer concept [23].

$$\psi_{k+1} = \left(\bar{E}^{-1} C_{k+1} P_{k+1|k} C_{k+1}^T S_{k+1}^{-1}\right)^{-1} \quad (3.5)$$

$$E = \left(\left|e_{z_{k+1|k}}\right|_{Abs} + \gamma \left|e_{z_{k|k}}\right|_{Abs}\right) \quad (3.6)$$

The values of (3.5) are compared with the limits for the smoothing boundary layer widths (a designer setting) to determine which gain is used (EKF or SVSF). If the values of (3.5) are larger than the limits (i.e., $\psi_{k+1} > \psi_{lim}$), the EK-SVSF gain is defined by [23]:

$$K_{k+1} = C^{+} diag\left[\left(\left|e_{z,k+1|k}\right|_{Abs} + \gamma \left|e_{z,k|k}\right|_{Abs}\right) \circ sat\left(\bar{\psi}^{-1} e_{z,k+1|k}\right)\right] diag\left(e_{z,k+1|k}\right)^{-1} \quad (3.7)$$

Otherwise, the EKF gain may be used (3.8). Note that this is a seamless transfer as the gain equation does not change drastically. Its amplitude changes smoothly as it crosses the boundary layer, ensuring continuity in the estimation process.

$$K_{k+1} = P_{k+1|k} C_{k+1}^T S_{k+1}^{-1} \quad (3.8)$$

Similar to the SVSF estimation process, the remaining part of the procedure includes updating the estimates (3.9) and the covariance (3.10). The measurement error, used in the next time step, is updated as per (3.11).

$$\hat{x}_{k+1|k+1} = \hat{x}_{k+1|k} + K_{k+1} e_{z,k+1|k} \quad (3.9)$$

$$P_{k+1|k+1} = (I - K_{k+1}C) P_{k+1|k} (I - K_{k+1}C)^T + K_{k+1} R_{k+1} K_{k+1}^T \quad (3.10)$$

$$e_{z,k+1|k+1} = z_{k+1} - h\left(\hat{x}_{k+1|k+1}\right) \quad (3.11)$$

IV. Experimental Setup and Results

A. Experimental Setup

An experimental brushless DC motor was used to obtain the results in this study. During the tests, the speed of the motor was fixed to 1,000 RPM without an external load. The angular position of the motor was measured using an absolute encoder. The phase voltages were obtained by direct line voltage measurements, and the corresponding phase currents were also obtained. All of the measurements were pre-processed with an anti-aliasing filter (500 Hz).

The motor was modeled as a third-order nonlinear system with six state variables related to its phase currents and phase resistances, respectively. The state estimates were initialized as zero. The sampling frequency of the system was f_T = 32,000 Hz. The discrete-time state equations are defined as follows [24-26].

$$x_{1,k+1} = -R_a^k \, dt/L_s \, x_{1,k} + \left(dt/L_s - K_e \Phi_{a,k}\right) u_k \quad (4.1)$$

$$x_{2,k+1} = -R_b^k \, dt/L_s \, x_{1,k} + \left(dt/L_s - K_e \Phi_{b,k}\right) u_k \quad (4.2)$$

$$x_{3,k+1} = -R_c^k \, dt/L_s \, x_{1,k} + \left(dt/L_s - K_e \Phi_{c,k}\right) u_k \quad (4.3)$$

$$x_{4,k+1} = x_{4,k} \quad (4.4)$$

$$x_{5,k+1} = x_{5,k} \quad (4.5)$$

$$x_{6,k+1} = x_{6,k} \quad (4.6)$$

Note that the state space vector is defined by $x_k = [I_a \quad I_b \quad I_c \quad R_a \quad R_b \quad R_c]_k^T$ and the input vector is defined as $u_k = [u_a \quad u_b \quad u_c \quad \omega \quad \theta_e]_k^T$. Furthermore, $\Phi_{a,k} = sin(\theta_e), \Phi_{b,k} = sin\left(\theta_e + \frac{2}{3}\pi\right), \Phi_{c,k} = sin\left(\theta_e - \frac{2}{3}\pi\right)$, and the relation between the electrical angle θ_e and the physical angle θ of the rotor is $\theta_e = 2P\theta$, P is the number of pole pairs and P = 4, $K_e = 0.77\ V \cdot s/rad$, and finally $L_s = 0.0048\ H$. The measurement equation is defined by:

$$z_{k+1} = C x_{k+1|k} \quad (4.7)$$

Note that for systems that have fewer measurements than states, a reduced order or Luenberger's approach is taken to formulate a full measurement matrix, as presented [21, 23, 27]. Essentially, 'artificial measurements' are created and used throughout the estimation process [23]. Similarly, in this case for the SVSF procedure, the artificial measurements of phase resistances are calculated using available measurements of voltage and current:

$$r_{MN} = \frac{u_{MN} - L\frac{di_{MN}}{dt} - K_{e2}\omega_{MN}}{i_{MN}} \quad (4.8)$$

Note that the subscript MN denotes the mean value of the variable in every half cycle, and K_{e2} is a voltage constant which is set to $0.4877\ V \cdot s/rad$. The signal r_{MN} was sent through a low-pass filter to create the artificial measurement. The modified measurement vector becomes:

$$z_{k+1} = [i_a \quad i_b \quad i_c \quad r_{MN,a} \quad r_{MN,b} \quad r_{MN,c}]_{k+1}^T \quad (4.9)$$

Furthermore, note that with (4.9), the measurement matrix in (4.7) becomes an identity. The system and measurement noise covariance was defined as a diagonal matrix, with the first three elements set to 1×10^{-5} and the last three elements set to 0.5×10^{-7}. The measurement matrix was also defined as a diagonal matrix, with the first three elements set to 1×10^{-3} and the last three elements set to 0.2. The initial state error covariance matrix was defined to be 100 times the system noise covariance. Furthermore, for the estimation process, the 'memory' or convergence rate was set to $\gamma = 0.2$. The limit set for the VBL was defined to be $\psi_{lim} = [2 \quad 2 \quad 2 \quad 300 \quad 300 \quad 300]^T$.

B. *Nonlinear Estimation Results*

Three different cases were studied. The first case was considered a normal condition, where no fault occurred in the motor. The second case included a faulty resistance in one of the phases of the motor. In the third case, a modeling error was injected in to the estimator half-way through the process, in order to test and compare the robustness of the EKF and EK-SVSF estimation methods. Figure's 3 and 4 show the resistance estimates for the EKF and EK-SVSF methods, respectively. Both methods were able to successfully obtain the correct values. However, note that the EK-SVSF converged faster toward the true state trajectory. This difference appears in the RMSE results for the normal case.

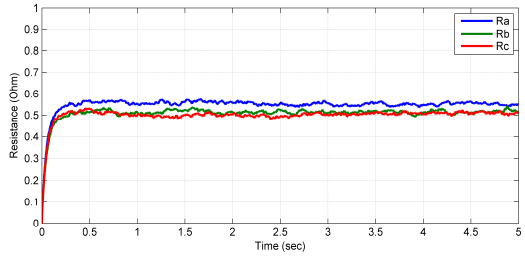

Figure 3. EKF estimation results (normal case).

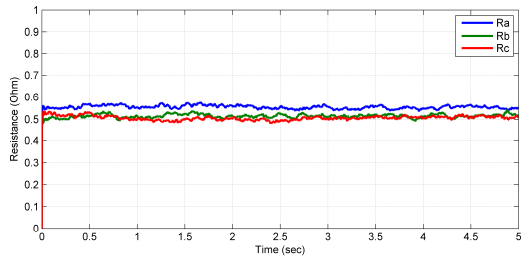

Figure 4. EK-SVSF estimation results (normal case).

The root mean square error (RMSE) results are summarized in the following table.

TABLE I. RMSE ESTIMATION RESULTS – NORMAL CASE

Filter	R_a	R_b	R_c
EKF	6.21×10^{-2}	3.83×10^{-2}	3.43×10^{-2}
EK-SVSF	5.46×10^{-2}	1.70×10^{-2}	1.16×10^{-2}

To simulate the winding resistance fault condition, an external resistor was added to the stator winding of the motor, doubling its resistance R_c halfway in the estimation process. The estimation results are shown in the following two figures.

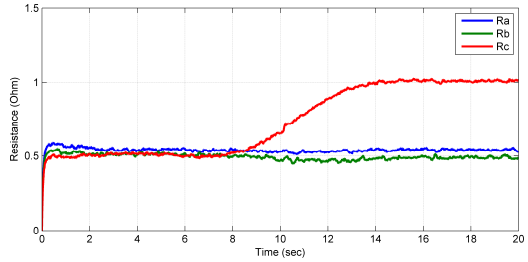

Figure 5. EKF estimation results (winding resistance fault).

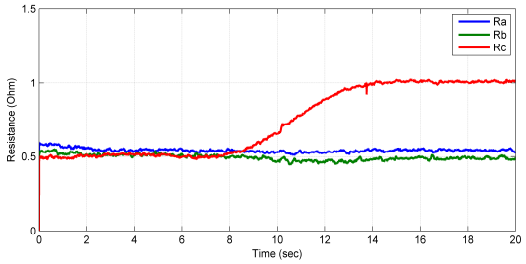

Figure 6. EK-SVSF estimation results (winding resistance fault).

As shown in Fig.'s 5 and 6, the EKF and EK-SVSF provides satisfactory results. The change in the resistance R_c from 0.5 Ohm to 1 Ohm was successfully captured, and the estimation of the other two phases are not affected by this disturbance. The reason that both methods yielded relatively the same results is that in the absence of modeling error, the SVSF gain is practically the same as that of the EKF. The resistance R_c was successfully tracked, and the estimation stabilized afterwards. The RMSE results are shown in the following table.

TABLE II. RMSE ESTIMATION RESULTS – WINDING RESISTANCE

Filter	R_a	R_b	R_c
EKF	4.53×10^{-2}	2.50×10^{-2}	3.31×10^{-1}
EK-SVSF	4.38×10^{-2}	1.94×10^{-2}	3.30×10^{-1}

The last case is used to compare the robustness of the filters under the presence of modeling uncertainties. As per [21], consider the introduction of a modeling error or uncertainty at 1.7 seconds into the test. The modeling uncertainty was introduced by decreasing the value of K_e in the model by 10%. The altered parameter was then changed back to the correct value at 3.3 seconds. The model used by the filters was changed; however, the actual conditions of the motor remained the same. The corresponding resistance estimates for this case are shown in the following figures.

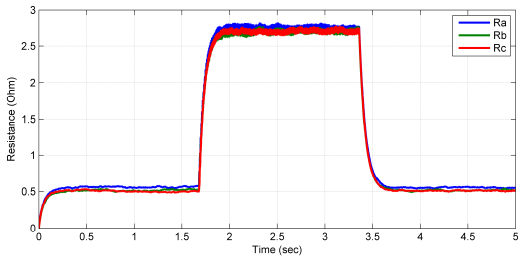

Figure 7. EKF estimation results (modeling error case).

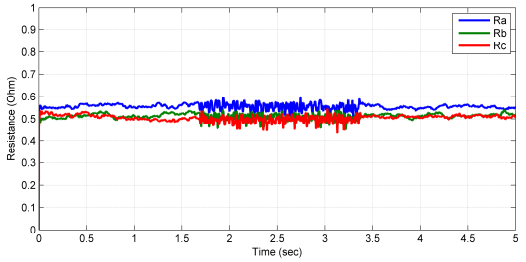

Figure 8. EK-SVSF estimation results (modeling error case).

The abrupt jump at 1.7 seconds is shown together with a sudden drop at 3.3 seconds. The estimation error of the EKF due to the modeling uncertainties is more than five times larger than the true value. However, the EK-SVSF estimation strategy was able to accurately estimate the resistance R_c during the presence of the fault and modeling error. All of the three states chattered among the true state trajectory when the modeling error was injected. The SVSF merit lies in its ability to minimize the influence of modeling errors while preserving stability. Furthermore, the changing width of the time-varying smoothing boundary layer (VBL) may be used to indicate the presence of un-modeled uncertainties or system faults, as shown in Fig. 9.

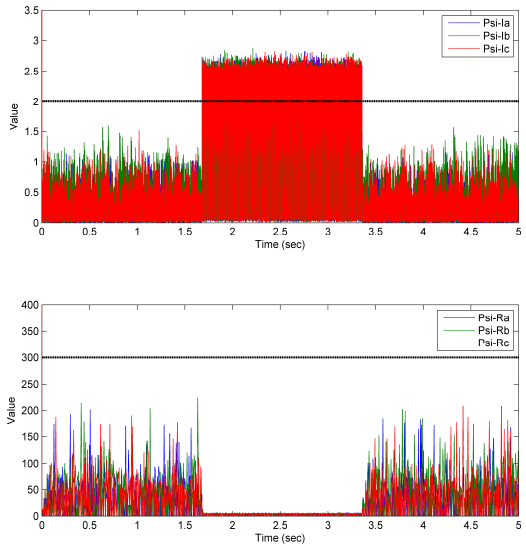

Figure 9. VBL results for $I_{a,b,c}$ and $R_{a,b,c}$ (modeling error case).

Although the estimates of the EK-SVSF method are not completely immune from the injected modeling error, the EK-SVSF results are significantly better than the EKF, as shown in the following table.

TABLE III. RMSE ESTIMATION RESULTS – MODELING ERROR

Filter	R_a	R_b	R_c
EKF	1.28	1.25	1.25
EK-SVSF	5.60×10^{-2}	1.78×10^{-2}	1.48×10^{-2}

V. CONCLUSIONS

The purpose of this paper was to study and compare the results of the EKF and EK-SVSF for the purposes of nonlinear estimation and fault detection. A brushless DC motor was used as the experimental apparatus. Experimental results demonstrated that both the EKF and EK-SVSF were able to provide accurate estimates under normal operating conditions. However, in the presence of modeling errors, the EKF completely deviated from the true state trajectories, while the EK-SVSF yielded accurate state estimates with a small magnitude of chattering. Moreover, the VBL width of the SVSF strategy was demonstrated to be a secondary indicator for system changes and modeling uncertainties.

APPENDIX

The following is a list of the main nomenclature used throughout the paper.

TABLE IV. LIST OF IMPORTANT NOMENCLATURE AND PARAMETERS

Parameter	Definition
f	Nonlinear system function
h	Nonlinear measurement function
x	State vector or values
z	Measurement (system output) vector or values
w	System noise vector
v	Measurement noise vector
A	Linear system transition matrix
B	Linear input gain matrix
C	Linear measurement (output) matrix
E	SVSF error vector (or matrix)
K	Filter gain matrix
P	State error covariance matrix
Q	System noise covariance matrix
R	Measurement noise covariance matrix
S	Innovation (measurement error) covariance matrix
e_z	Measurement (output) error vector
γ	SVSF 'memory' or convergence rate
ψ	SVSF smoothing boundary layer
$diag[a]$ or $\bar{a}$	Diagonal of some vector or matrix a
$sat()$	Saturation function
$\|a\|$	Absolute value of a
T	Transpose of a vector (if superscript) or sample rate
$+$	Pseudoinverse of some non-square matrix
$\circ$	Denotes a Schur product (element-by-element multiplication)
$\sim$	Denotes error or difference
$\hat{}$	Estimated vector or values

REFERENCES

[1] A. H. Bonnett and C. Yung, "Increased efficiency versus increased reliability - A comparison of pre-EPAct, EPAct, and premium-efficient motors," *Ieee Industry Applications Magazine,* vol. 14, pp. 29-36, Jan-Feb 2008.

[2] A. Bellini, F. Filippetti, C. Tassoni, and G. A. Capolino, "Advances in Diagnostic Techniques for Induction Machines," *Ieee Transactions on Industrial Electronics,* vol. 55, pp. 4109-4126, Dec 2008.

[3] C. H. De Angelo, G. R. Bossio, S. J. Giaccone, M. I. Valla, J. A. Solsona, and G. O. Garcia, "Online Model-Based Stator-Fault Detection and Identification in Induction Motors," *Ieee Transactions on Industrial Electronics,* vol. 56, pp. 4671-4680, Nov 2009.

[4] G. Kenne, T. Ahmed-Ali, F. Lamnabhi-Lagarrigue, and A. Arzande, "Nonlinear systems time-varying parameter estimation: Application to induction motors," *Electric Power Systems Research,* vol. 78, pp. 1881-1888, Nov 2008.

[5] M. Messaoudi, L. Sbita, and M. N. Abdelkrim, "A robust nonlinear observer for states and parameters estimation and on-line adaptation of rotor time constant in sensorless induction motor drives," *International Journal of Physical Sciences,* vol. 2, pp. 217-225, Aug 2007.

[6] R. Wierzbicki and C. T. Kowalski, "Application of an extended Kalman filter for stator fault diagnosis of induction motor," *Przeglad Elektrotechniczny,* vol. 86, pp. 82-86, 2010.

[7] H. Kim, "On-line mechanical unbalance estimation for permanent magnet synchronous machine drives," *Iet Electric Power Applications,* vol. 3, pp. 178-186, May 2009.

[8] S. H. Said, M. F. Mimouni, F. M'Sahli, and M. Farza, "High gain observer based on-line rotor and stator resistances estimation for IMs," *Simulation Modelling Practice and Theory,* vol. 19, pp. 1518-1529, Aug 2011.

[9] L. Romeral, J. C. Urresty, J. R. R. Ruiz, and A. G. Espinosa, "Modeling of Surface-Mounted Permanent Magnet Synchronous Motors With Stator Winding Interturn Faults," *Ieee Transactions on Industrial Electronics,* vol. 58, pp. 1576-1585, May 2011.

[10] K. H. Kim, D. U. Choi, B. G. Gu, and I. S. Jung, "Fault model and performance evaluation of an inverter-fed permanent magnet synchronous motor under winding shorted turn and inverter switch open," *Iet Electric Power Applications,* vol. 4, pp. 214-225, Apr 2010.

[11] H. Fakham, M. Djemai, and K. Busawon, "Design and practical implementation of a back-EMF sliding-mode observer for a brushless DC motor," *Iet Electric Power Applications,* vol. 2, pp. 353-361, Nov 2008.

[12] S. Bolognani, R. Oboe, and M. Zigliotto, "Sensorless full-digital PMSM drive with EKF estimation of speed and rotor position," *Ieee Transactions on Industrial Electronics,* vol. 46, pp. 184-191, Feb 1999.

[13] B. Murat, B. Seta, and G. Metin, "Speed-Sensorless Estimation for Induction Motors Using Extended Kalman Filters," *Industrial Electronics, IEEE Transactions on,* vol. 54, pp. 272-280, 2007.

[14] O. Moseler and R. Isermann, "Application of model-based fault detection to a brushless DC motor," *Ieee Transactions on Industrial Electronics,* vol. 47, pp. 1015-1020, Oct 2000.

[15] T. Boileau, B. N. Mobarakeh, and F. M. Tabar, "On-line Identification of PMSM Parameters: Model-Reference vs EKF," *2008 Ieee Industry Applications Society Annual Meeting, Vols 1-5,* pp. 1410-1417, 2008.

[16] S. Bolognani, M. Zigliotto, and K. Unterkofler, "On-line parameter commissioning in sensorless PMSM drives," in *Industrial Electronics, 1997. ISIE '97., Proceedings of the IEEE International Symposium on*, 1997, pp. 480-484 vol.2.

[17] B. Terzic and M. Jadric, "Design and implementation of the extended Kalman filter for the speed and rotor position estimation of brushless DC motor," *Industrial Electronics, IEEE Transactions on,* vol. 48, pp. 1065-1073, 2001.

[18] A. Masi, M. Butcher, M. Martino, and R. Picatoste, "An Application of the Extended Kalman Filter for a Sensorless Stepper Motor Drive Working With Long Cables," *Ieee Transactions on Industrial Electronics,* vol. 59, pp. 4217-4225, Nov 2012.

[19] L. Liu and D. A. Cartes, "On-line identification and robust fault diagnosis for nonlinear PMSM drives," *ACC: Proceedings of the 2005 American Control Conference, Vols 1-7,* pp. 2023-2027, 2005.

[20] A. Gandhi, T. Corrigan, and L. Parsa, "Recent Advances in Modeling and Online Detection of Stator Interturn Faults in Electrical Motors," *Ieee Transactions on Industrial Electronics,* vol. 58, pp. 1564-1575, May 2011.

[21] S. Habibi, "The Smooth Variable Structure Filter," *Proceedings of the IEEE,* vol. 95, pp. 1026-1059, 2007.

[22] S. A. Gadsden, S. R. Habibi, T. Kirubarajan, "Kalman and Smooth Variable Structure Filters for Robust Estimation," *IEEE Transactions on Aerospace and Electronic Systems,* 2012.

[23] S. A. Gadsden, "Smooth Variable Structure Filtering: Theory and Applications," McMaster University, Open Access Dissertations and Theses, 2011.

[24] M. S. Z. Abidin and R. Yusof, "Application of a model-based fault detection and diagnosis using parameter estimation and fuzzy inference to a DC-servomotor," *Proceedings of the 2002 Ieee International Symposium on Intelligent Control,* pp. 783-788, 2002.

[25] O. Moseler and R. Isermann, "Model-based fault detection for a brushless DC motor using parameter estimation," *Iecon '98 - Proceedings of the 24th Annual Conference of the Ieee Industrial Electronics Society, Vols 1-4,* pp. 1956-1960, 1998.

[26] R. Isermann, "Model-based fault-detection and diagnosis - status and applications," *Annual Reviews in Control,* vol. 29, pp. 71-85, 2005.

[27] D. G. Luenberger, *Introduction to dynamic systems: theory, models, and applications*: Wiley, 1979.